SPATIAL DISTRIBUTION AND TEMPORAL EVOLUTION OF CORONAL BRIGHT POINTS

JIE ZHANG[1], MUKUL R. KUNDU and STEPHEN M. WHITE
Department of Astronomy, University of Maryland, College Park, MD 20742, U.S.A.

(Received 23 May 2000; accepted 20 September 2000)

Abstract. We present a statistical study of the spatial distribution and temporal evolution of coronal bright points (BPs) by analyzing a continuous set of observations of a quiet-Sun region of size $780'' \times 780''$ over a period of 55 hours. The main data set consists of observations taken by EIT (the Extreme-ultraviolet Imaging Telescope on board the SOHO spacecraft) in its Fe XII 195 Å channel which is sensitive to coronal plasma of temperature ~ 1.5 MK; we also use soft X-ray observations by SXT (Soft X-ray Telescope on the *Yohkoh* spacecraft) which is sensitive to coronal plasma of temperature > 2.5 MK. The flux histogram for all pixels in EIT 195 Å images indicates that BPs have a power law flux distribution extending down to a level of 3σ (σ, root mean square deviation) above the average flux of the quiet Sun, while the bulk quiet Sun has a Gaussian-like flux distribution. Using a 3σ intensity threshold, we find a spatial density of one BP per 90 Mm $\times$ 90 Mm area, or equivalently 800 BPs for the entire solar surface at any moment. The average size of a BP is 110 Mm^2. About 1.4% of the quiet-Sun area is covered by bright points and the radiation from all BPs is only about 5% of that from the whole quiet Sun. Thus, the atmosphere above quiet-Sun regions is not energetically dominated by BPs. During the 55-hour period of EIT observations, we identify 48 full-life-cycle BPs which can be tracked from their initial appearance to final disappearance. The average lifetime of these BPs is 20 hours, which is much longer than the previously reported 8 hours based on *Skylab* X-ray observations (Golub *et al.*, 1974). We also see shorter life times and smaller numbers of BPs in the soft X-ray images than in the EIT 195 Å observations, suggesting that the temperature of BPs is generally below 2 MK.

1. Introduction

Coronal bright points (hereafter BPs) are identified as small ($< 60''$) and short-lived (< 2 days) coronal features with enhanced emission, which are located mostly in quiet-Sun regions and coronal holes. The large number of BPs in the corona make them an important aspect of coronal structure and dynamics, and their relatively simple structure allows them to be easily studied. They were first discovered in X-ray observations in the early 1970s (Vaiana *et al.*, 1973). Golub *et al.* (1974) studied the properties of BPs at X-ray wavelengths and found a mean life-time of 8 hours from the *Skylab* observations. During its life, a BP often shows very irregular variations in intensity and shape on time scales of a few minutes (Sheeley and Golub, 1979; Habbal and Withbroe, 1981; Habbel, Dowdy, and Withbroe, 1990;

[1]Center for Earth Observing and Space Research, Institute for Computational Science, George Mason University, Fairfax, VA 22030, U.S.A.

Solar Physics **198:** 347–365, 2001.

Strong *et al.*, 1992; Krucker *et al.*, 1997; Benz and Krucker, 1999; Shimojo and Shibata, 1999); the intermittent nature of BPs has been suggested to arise from micro-flares, the strongest of which provide evidence for non-thermal electrons as indicated by the occurrence of metric type III radio bursts (e.g., Kundu *et al.*, 1995). In spite of the large number of BPs, they occupy only a small part of the solar surface, and thus their summed radiation energy is much smaller than that of the background quiet Sun (Habbal and Grace, 1991; Habbal, 1992; Falconer *et al.*, 1998). Coronal BPs are associated with regions of mixed polarity flux of magnetic network (Harvey, Harvey, and Martin 1975; Webb *et al.*, 1993; Harvey, 1996; Kankelborg *et al.*, 1996; Falconer *et al.*, 1998; Pres and Phillips, 1999). Detailed theoretical modeling of BPs has been carried out based on the magnetic reconnection of cancelling magnetic features (Priest, Parnell, and Martin, 1994; Longcope, 1998).

In this paper, we examine BPs at EUV and soft X-ray wavelengths in order to investigate their spatial distribution and temporal evolution by continuously tracking a large quiet-Sun region over a long period. The EUV observations were obtained by EIT (Extreme-ultraviolet Imaging Telescope on SOHO, Delaboudinière *et al.*, 1995) in its Fe XII 195 Å channel which is sensitive to coronal plasma of temperature $\sim$ 1.5 MK, while soft X-ray observations were made by SXT (Soft X-ray Telescope on *Yohkoh*, Tsuneta *et al.*, 1991) which is sensitive to coronal plasma $>$ 2.5 MK. Although comparable in spatial and temporal resolution with previous investigations, our data sets are much better in terms of spatial and temporal extent. This advantage enables us to make significant statistical studies based on a large number of BP events. In particular, we are able to determine the lifetime of BPs in EUV observations, and the result turns out to be much different from the early study in X-rays (Golub *et al.*, 1974). In Section 2, we present the observations. In Section 3 we present the analysis and results. The discussions and conclusions are given in Sections 4 and 5, respectively.

2. Observations

We use mainly the EIT observations to study coronal bright points. SXT observations are also used as a comparison, which will be presented in detail in Section 3. EIT, a normal-incidence telescope with multi-layer-coated mirrors, observes the Sun in four narrow EUV channels centered at 171 Å, 195 Å, 284 Å and 304 Å which selectively observe strong spectral lines formed by Fe IX/X, Fe XII, Fe XV, and He II, respectively; the temperatures of maximum ionization fraction of the ions are 1.0 MK, 1.5 MK, 2.1 MK, and 0.08 MK, respectively. The images are taken on an EUV-sensitive 1024 $\times$ 1024 format charge coupled device (CCD) camera with a pixel size of 2.6″ and a field of view of 45′ $\times$ 45′, which results in an effective spatial resolution of 5.2″ and full view of the Sun extending up to 1.5 $R_{\odot}$. In the Synoptic Watch Plan (the so-called Coronal Mass Ejection Watch

Plan), EIT continuously takes images in the 195 Å channel approximately every 20 min, while it takes images in the other three channels every six hours. Since the SOHO spacecraft is located at the L1 vantage point between the Earth and the Sun, the observations are continuous and not interrupted by satellite night as for Earth-orbiting spacecraft. This type of full disk, high spatial resolution, modest cadence and continuous observation of the Sun offers us an excellent opportunity to trace the life cycle of numerous EUV bright points in the corona. Note that we only use observations in the EIT 195 Å channel due to poor cadence in the other three channels. However, it turns out that the 195 Å channel is the best to observe coronal BPs among all EIT channels, as is evident from the observations.

Out of the vast number of EIT synoptic observations since the launch of SOHO in December 1995, we pick three days of observations made in November 1997 (in the rising phase of solar cycle 23) for our BP study. This study could easily be repeated with similar data sets from other periods. The data we choose are the observations from 15 UT, 10 November to 22 UT, 12 November with a temporal extent of 55 hours. During this period, there are in total 130 EIT 195 Å images taken (each image is a snapshot with exposure time of $\sim$ 5 s). We finally use 125 images in our analysis, since the other 5 images are poor in quality for instrumental reasons. The time intervals between two adjacent images lie mostly (113 out of 124 cases) in the range of 10 to 35 min. It turns out that the effective temporal resolution is 26 min.

In Figure 1, we show the EIT 195 Å image taken at 18:46 UT, 11 November, 1997 which is in the middle of our tracking period; the sequence number of this image is 61. The solid-line box in the middle of the disk indicates the region we are interested in; its size is 300 $\times$ 300 pixels or 780″ $\times$ 780″. Since EIT always points at the Sun's center in the full-disk observational mode, we need to carry out a rotational correction in order to align the region of interest for preceding and following images. The Sun is rotating at a rate of about 10″ per hour at the center, and the rate decreases towards the limb due to projection effects. The dotted-line box to the left shows the location of the region of interest at the time of the first image in the sequence (15:36 UT, 10 November), while the broken-line box to the right shows the location of the region of interest in the last image (22:51 UT, 12 November). The rectangles together trace a region of 1150″ across, or about $\frac{2}{3}$ of the Sun's angular diameter. Our chosen region of interest always lies well on the disk in the 55-hour-long period. Thus, the distortion caused by projection should be minimized. Since the lifetime of bright points is well below 55 hours, our data set is long enough to track many bright points through their life cycle.

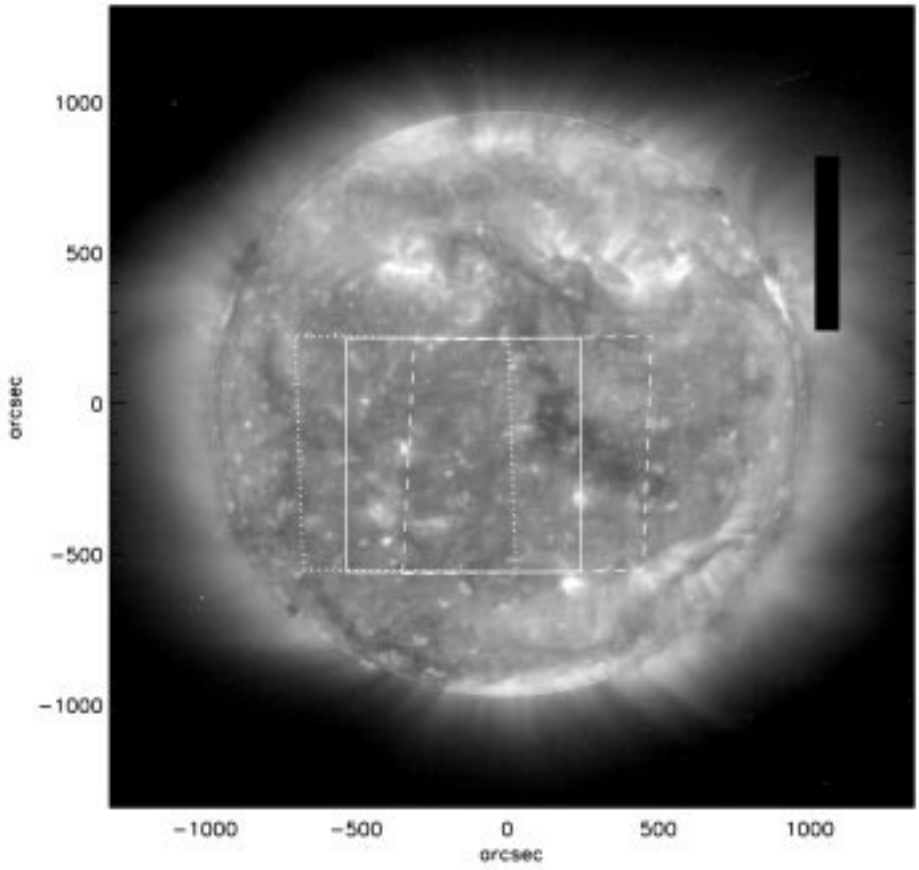

Figure 1. EIT snapshot image of the Sun in the 195 Å channel taken at 18:46 UT, 11 November, 1997. The box denoted by the *solid line* indicates the solar region we are interested in for the study of bright points. The left and right boxes denoted by *dotted lines* indicate the same solar region at the times of 15:36 UT, 10 November and 22:51 UT, 12 November, respectively; the difference of the location is caused by the rotation of the Sun. The Sun's north is to the top, and east is to the left.

3. Analysis and Results

3.1. Identification of bright points

Figure 2 shows the image of the region of interest (a part of the image of 18:46 UT, 11 November in Figure 1) on which we identify 41 BPs as indicated by rectangular boxes. A BP, though point-like looking in a full Sun image, is actually a compact, enhanced region which is often a resolved loop-like structure and may include many pixels in the observations. As shown in the image, there are numerous sources which should be regarded as bright points according to the definition. The strong sources can be identified unambiguously. However, the question arises when

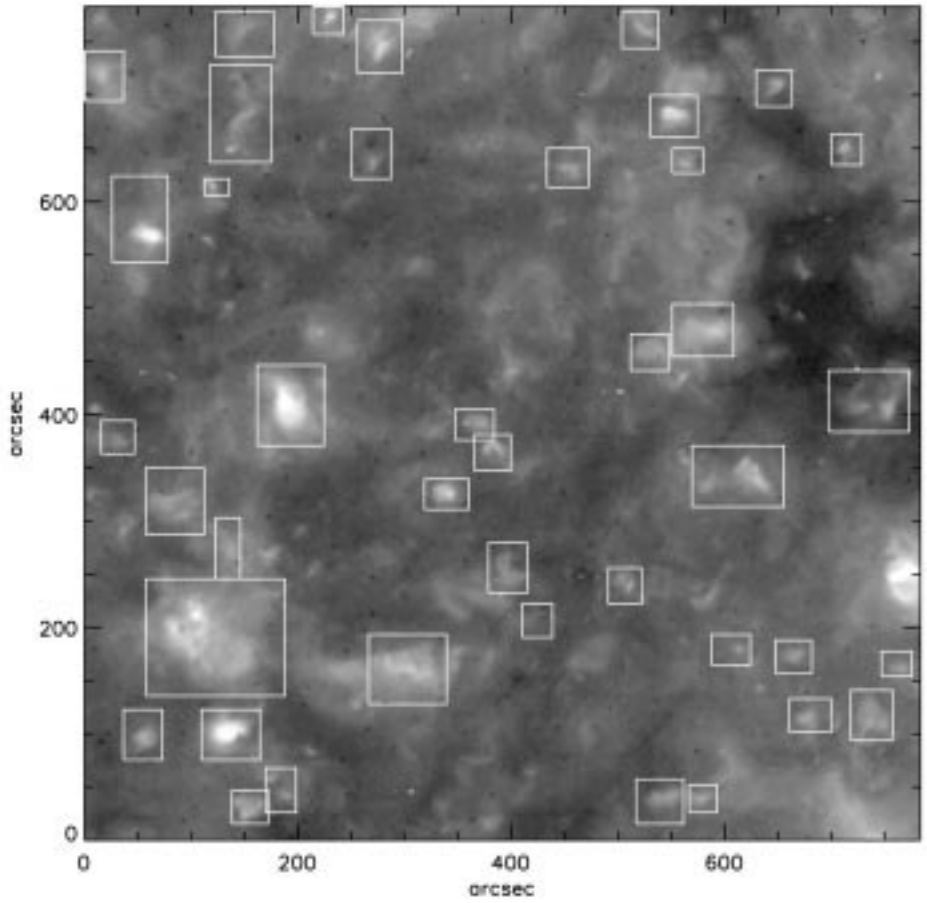

Figure 2. Identified coronal bright points in the quiet-Sun region of interest. The image, taken at 18:46 UT, 11 November, 1997 in the EIT 195 Å channel, shows a quiet-Sun region of size 780″ (the region in the box of Figure 1). The boxes indicate the locations of 41 identified bright points.

one examines the fainter sources: there always exist fainter and fainter sources which eventually become indistinguishable from the bulk of the quiet Sun. In order to conduct our statistical studies, it is necessary to set up a quantitative criterion to select BPs from the bulk quiet Sun. We adopt a 3σ intensity threshold to define a BP; σ is the standard rms (root mean square) deviation of the flux for the entire quiet-Sun region.

The 3σ threshold seems to have some physical significance in differentiation of features in quiet-Sun regions. Of a total of 9×10^4 EIT pixels in that region, the average flux is 55.2 DN s $^{-1}$ pixel^{-1} and the standard deviation σ is 26.7 DN s^{-1}pixel^{-1}. Thus, the flux of 3σ above the average is 135.3 DN s^{-1}pixel^{-1}. In Figure 3, we show a histogram of flux values for the 9×10^4 EIT pixels in the region. The histogram curve can be decomposed into two components: a Gaussian-

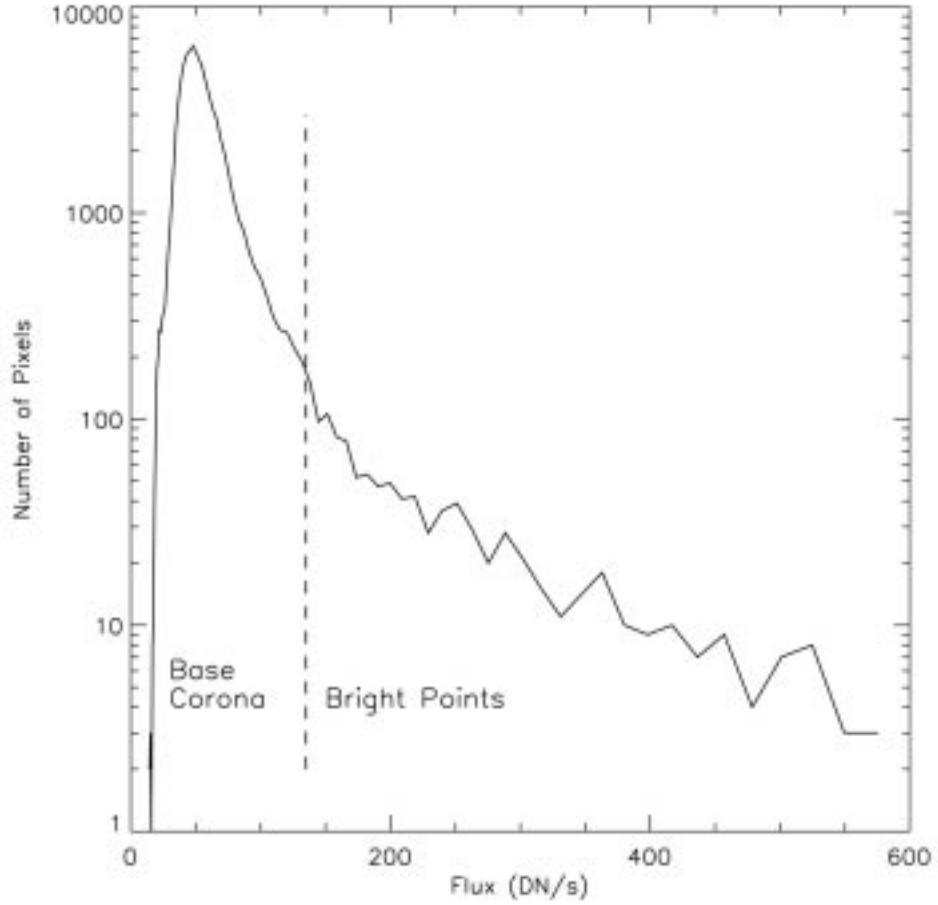

Figure 3. Flux histogram (*solid line*) of the quiet-Sun region of interest (see Figure 2). The vertical *dotted line*, which happens to separate the Gaussian-like part to the left and power-law part to the right, indicates the position of 3σ above the average flux of the quiet Sun.

like distribution at lower flux values (the part to the left of the vertical dotted line) and a power-law distribution at higher flux values (the part to the right of the dotted vertical line). The dotted vertical line indicates the position of 3σ deviation above the average flux. It is obvious that the 3σ line separates the Gaussian-like distribution and the power-law distribution. The power-law part is composed of the enhanced features in the quiet-Sun regions, mostly the BPs, while the Gaussian-like part is from the bulk quiet-Sun pixels which we define as the base corona. The base corona flux distribution (the Gaussian-like part) has a peak flux at 48 DN s^{-1}pixel^{-1} and a minimum flux at 10 DN s^{-1} pixel^{-1}. The flux distribution of BPs (power-law-like part) is in the range of 135 to 600 DN s^{-1} pixel^{-1}, 3 to 12 times higher than the typical quiet-Sun flux value.

3.2. SPATIAL DISTRIBUTION OF BRIGHT POINTS

Based on a 3σ intensity threshold, we have identified 41 BPs in the region of size $780'' \times 780''$ as shown in Figure 2. On the average, the spatial density of BPs is one every $120'' \times 120''$, or one every 90 Mm $\times$ 90 Mm area. Extending to the entire solar surface, there would be about 800 BPs at any one moment.

The coverage in area of all BP pixels ($>3\sigma$) is 1.4%, which gives the average size for a BP of 110 Mm^2, or $14'' \times 14''$ if the BP is of a square shape. However, BPs show a broad range of spatial size and shape, and most of them are observed to have an elongated configuration. The length is usually in the range of $10''$ to $30''$ with a maximum at $50''$. Certainly, the size of a BP changes with its evolutionary state since we set a strict intensity threshold: it is smaller in the rising and decaying phases and largest in its peak phase. Therefore, a more quantitative approach to determine the size distribution of BPs is to measure the size at their peak times, not just using a snapshot image as we have done here.

Although BPs are coronal structures of enhanced brightness, their total emission output is relatively small compared to the total emission output of the whole quiet-Sun region, due to their small filling factor on the disk. It is found that the total flux of pixels $> 3\sigma$ is 5.2% of the total flux of that region, while the area covered by these pixels is 1.4% of the total area. For all pixels $> 2\sigma$ (or flux $>$ 108.6 DN s^{-1} $pixel^{-1}$), the emission and area coverage are 8.3% and 2.8% of that of the entire region respectively. For all pixels $> 1\sigma$ (or flux $>$ 81.9 DN s^{-1} $pixel^{-1}$), the emission and area coverage are 16.1% and 7.5% of the region, respectively. Apparently, the energy output from the BPs themselves, even combined with regions surrounding BPs or of decaying BPs, is only a small part of the total energy output of the quiet Sun. Although these numbers are derived from a particular observation at 18:46 UT, 11 November, 1997, we find that they are in rather good agreement with the observations at other times.

3.3. TEMPORAL EVOLUTION OF BRIGHT POINTS

In a movie presentation of the 125 sequences of coronal images covering the period of 55 hours (see the CD-ROM), we clearly see that BPs come and go and are randomly distributed in the quiet-Sun region. This type of distribution has also been found in many earlier studies. As an example, in Figure 4 we show 4 snapshot images taken at 15:36 UT, 10 November (sequence 1, upper-left panel), 07:54 UT, 11 November (sequence 33, upper-right panel), 22:39 UT, 11 November (sequence 72, lower-left panel) and 14:27 UT, 12 November (sequence 103, lower-right panel), which are about 0, 16, 31, and 47 hours later than the first image, respectively. The difference of appearance from image to image is obvious. Indeed, the BPs evolve on a time scale of hours. The BP pattern at the end of our tracking period is totally different from that in the beginning; none of the BPs persists through the entire 55-hour period.

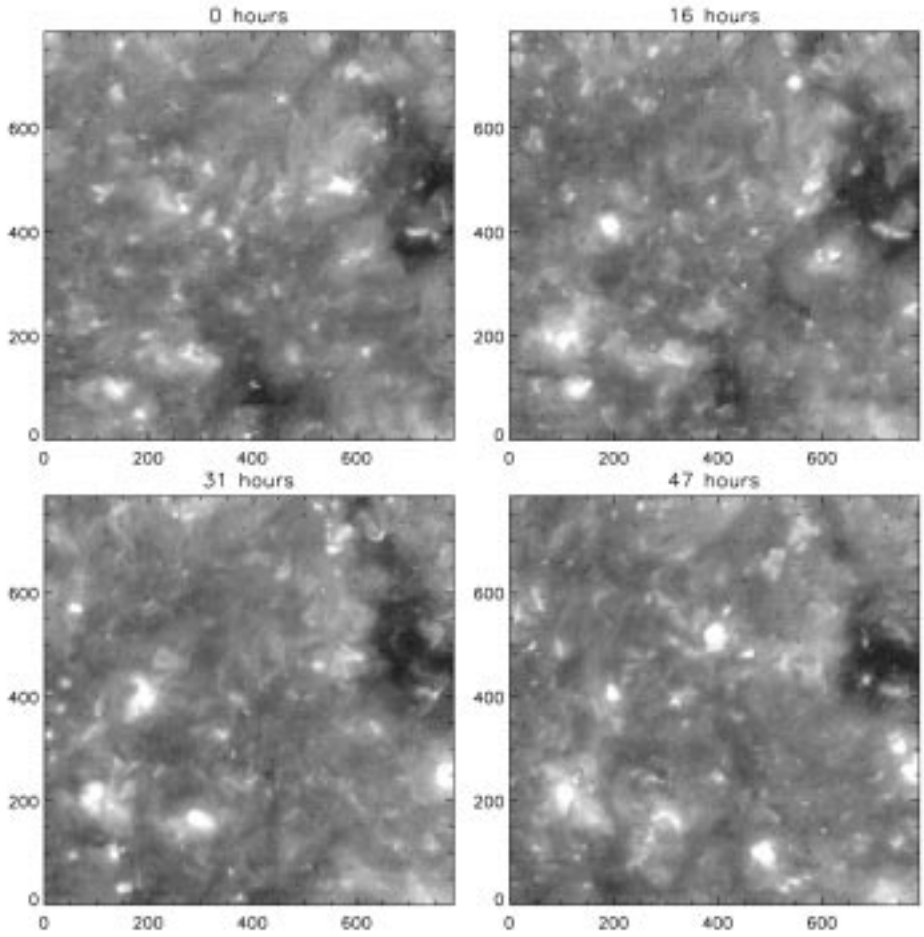

Figure 4. A set of quiet-Sun images of the same region taken at four different times in the EIT 195 Å channel showing the evolution of the pattern of coronal bright points. The four images, upper-left, upper-right, lower-left and lower-right are taken at 15:36 UT, 10 November, 07:54 UT, 11 November, 22:39 UT, 11 November, and 14:27 UT, 12 November, respectively. The number at the top of each image indicates the elapsed time from the first image.

In the following studies, we concentrate on the BPs whose full life cycle can be tracked during the EIT observations in order to study their evolution. A full-cycle BP should display its initial appearance or birth, growth, decay, and disappearance during the 55-hour tracking period. Based on this criterion, we identify 48 such BPs. In Figure 5, the locations of these 48 full-cycle BPs are labeled; the numbering is in the descending order of the peak flux of the events. The image displayed is the snapshot image at 18:46 UT, 11 November, as in Figure 2, which now serves as the reference for the position of the full-cycle BPs. Indeed, there are at least 150 distinct BPs showing up in the 125 images; however, about $\frac{2}{3}$ of them either

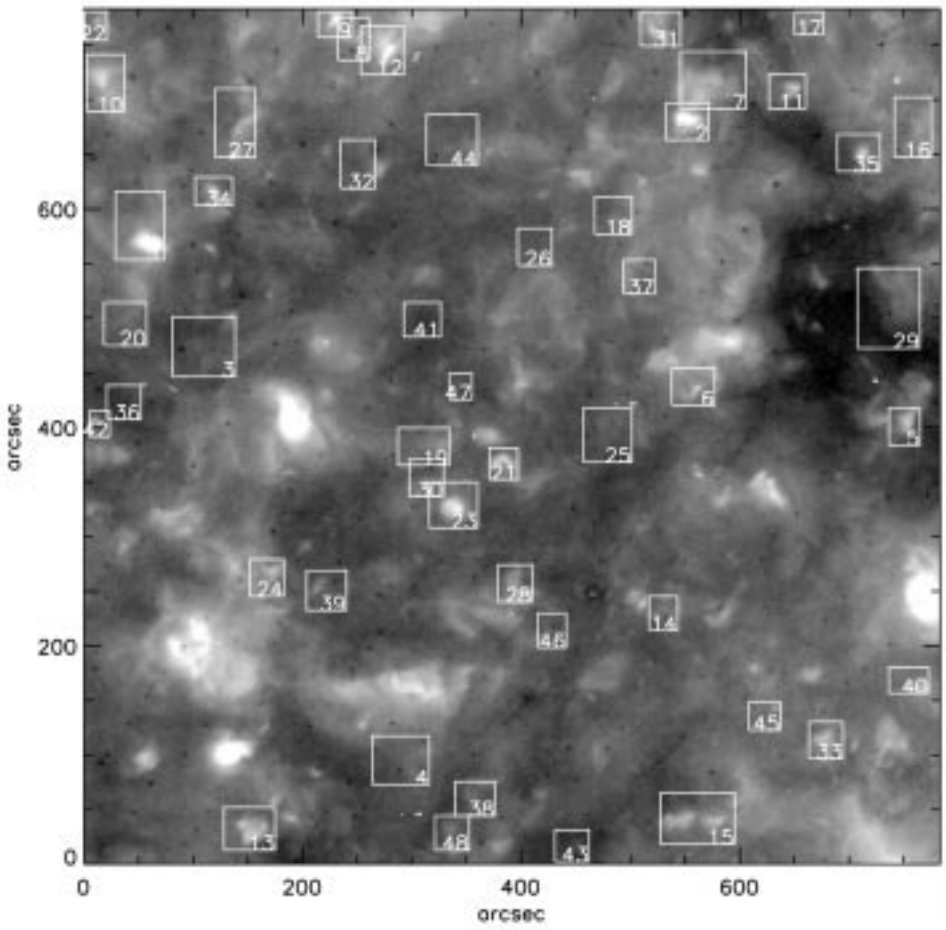

Figure 5. Bright points identified with full life cycle track. The numbered boxes indicate the location of these events (total 48 events). The numbering is in the order of descending strength of BPs at their peak. The background image is the same as in Figure 2.

have already appeared at the beginning of the tracking period and disappear later, or appear later and survive beyond the last frame. These BPs with only partial coverage are excluded from our analysis.

We display the evolution of two individual BPs, as representative of the 48 full-cycle BPs, in Figures 6 and 7 (events numbered 1 and 4 in Figure 5) respectively. In each figure, the number in each frame shows the elapsed time relative to the first frame in units of hours (H). The time goes from left to right and top to bottom. In Figure 6, we display 81 frames for event 1 from 05:15 UT, 11 November to 16:53 UT, 12 November. This event has a rising phase of about 3 hours: it starts to appear at 4.8 H (hour) and keeps increasing until 7.9 H. It then maintains a high flux level for 10 hours until 17.3 H followed by a flux dip lasting about 4 hours. It

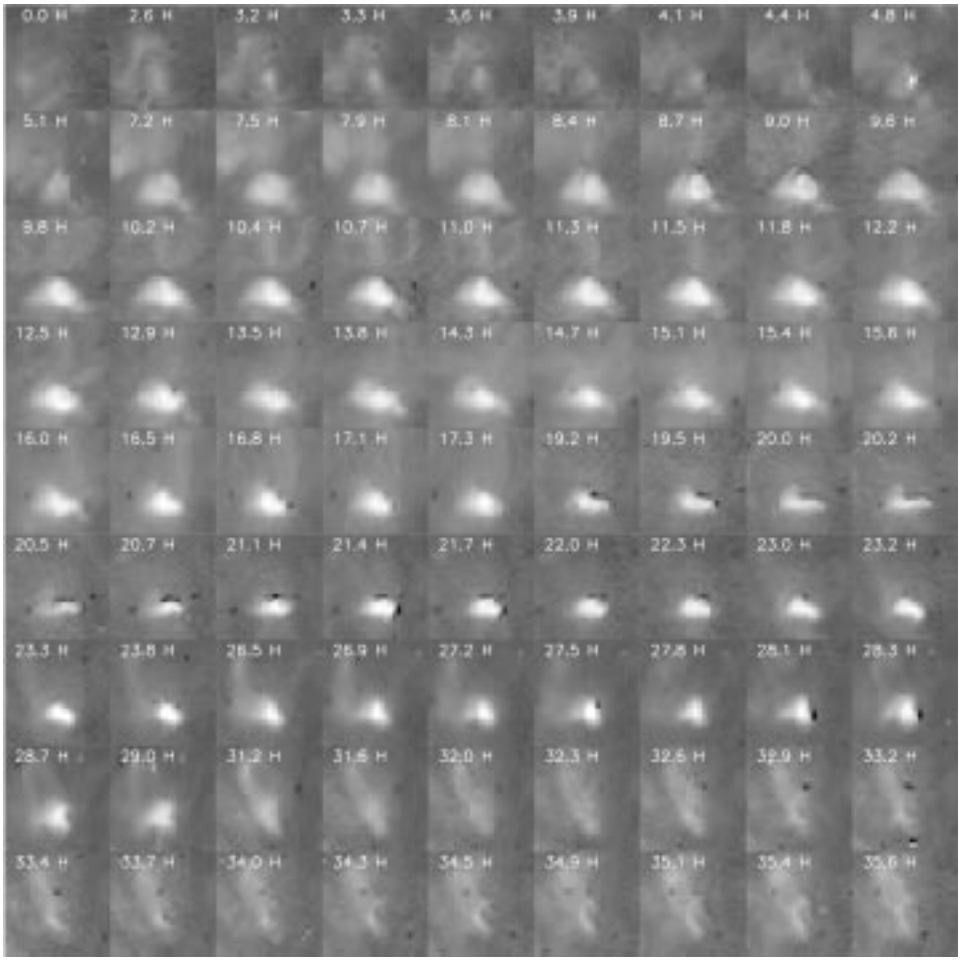

Figure 6. 81-image sequence showing the evolution of the bright point numbered 1 in Figure 5. The size of the displayed field is 65″. The first and last frames correspond to times of 05:15 UT, 11 November and 16:53 UT, 12 November, 1997, respectively. The number in each frame shows the elapsed time relative to the first frame in units of H (hour). The time goes from left to right and top to bottom.

regains its strength at 21.4 H and lasts for about 7 hours until 29.0 H followed by a rapid decay which leads to the disappearance of the event within 3 hours. The total lifetime of event 1 is about 27 hours. This BP has a compact round loop shape; its size varies from 30″ in its strong phase to 20″ in its weak phase.

In Figure 7, event 4 is shown in 49 frames covering from 16:59 UT, 10 November to 15:44 UT, 11 November. It is a strong event with a peak flux at 420 DN s^{-1} $pixel^{-1}$. It has a rising phase of < 3.2 hour, which is evident from the sharp difference between the images in the first and second frames. It then maintains a bright level phase for about 9 hours until 12.2 H. It decays within 3 hours and disappears

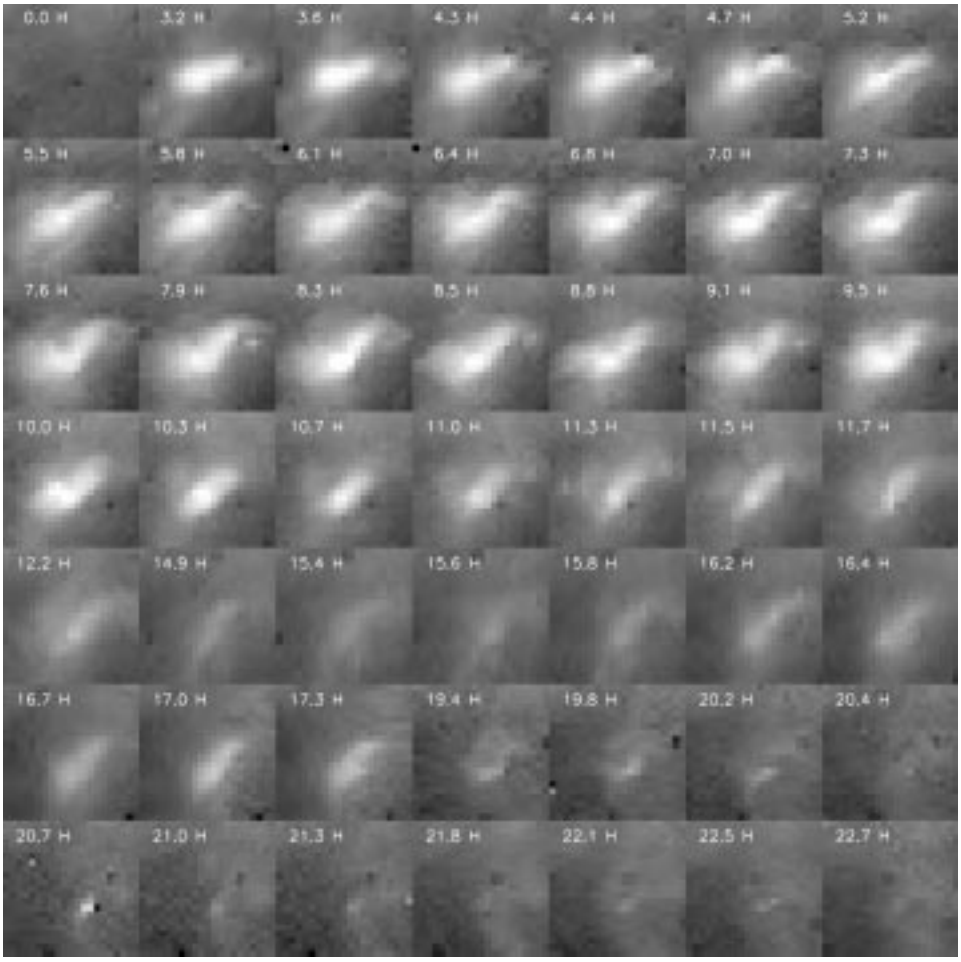

Figure 7. 49 image sequence showing the evolution of the bright point numbered 4 in Figure 5. The size of the displayed field is 52″. The first and last frames correspond to a times of 16:59 UT, 10 November and 15:44 UT, 11 November 1997, respectively. The number in each frame shows the elapsed time relative to the first frame in units of H (hour). The time goes from left to right and top to bottom.

at 15.4 H. The total lifetime of this BP is about 14 hours. However, at the same location, another weaker BP shows up just half an hour later and lasts for about 5 hours. Both the earlier and later BPs have an elongated loop structure with a length of 40″ and width of 10″.

3.4. LIFETIME OF BRIGHT POINTS

In Figures 8 (BPs numbered from 1 to 24 in Figure 5) and 9 (BPs numbered from 25 to 48 in Figure 5), we show the time profiles of the 48 full-cycle events which are sequenced in the descending order of their peak flux. In each panel, the X-axis

indicates the time ranging from 0 to 60 hours; the Y-axis indicates the flux of the peak pixel of the BP in the snapshot images. Note that the maximum labeled fluxes on the Y-axis are 800 DN s $^{-1}$ pixel^{-1} and 300 DN s $^{-1}$ pixel^{-1} for Figures 8 and 9, respectively. The number in the upper-left of each panel indicates the numbering of BPs in Figure 5 which shows their location.

The time profiles demonstrate the complex evolution of BPs. The most obvious feature is the spiky pattern which occurs through the life of a BP. The spikes are more apparent in the time profiles of weaker events. The duration of the spikes is usually as short as the temporal resolution limit of the observations, or about 26 min. This result of fast fluctuation of BPs is consistent with many earlier studies mentioned in the introduction of this paper.

Nevertheless, the spikes are superposed on a smooth profile whose trend defines the long term evolution of BPs. We now determine the lifetime of BPs based on their long term profiles. A typical long term profile is composed of three phases: a fast rising phase, a relatively long main phase and a fast decaying phase. A good example is seen in event 1, whose rising phase is about 3 hours, main phase about 21 hours and decaying phase is about 3 hours with a total lifetime of 27 hours. It is relatively straightforward to determine the lifetime of BPs (birth to death) from the time profiles in Figures 8 and 9.

In Figure 10, we plot the histogram of the lifetimes of the 48 full-cycle events. There is an apparent peak at about 20 hours. The lifetime of the 48 events ranges from a minimum of 5 hours to a maximum of 40 hours; 36 out of the 48 events have a lifetime between 10 and 30 hours. The average lifetime of the 48 events is 20 hours with a standard deviation of 8 hours. The significance of the numbers will be discussed in Section 4.

3.5. Comparison with SXT observations

Above we have studied coronal BPs based on EIT 195 Å observations which are sensitive to coronal plasma with temperature $\sim$ 1.5 MK. In this section we investigate these same BPs in a higher temperature range ($>$ 2.5 MK) using soft X-rays observed by SXT. Full-Sun images are continuously taken by SXT during the 55 hour period in half resolution mode (4.9$''$ pixels) alternatively using thin Al and AlMg filters. Unfortunately, the observations in the last 15 hours (from 07 UT to 22 UT, 12 November) are poor for instrumental reasons. Nevertheless, we are able to compare the observations with EUV during the first 40 hours. There are in total 37 valid snapshot images with the thin Al filter and 40 images with the AlMg filter observations with sufficient exposure time to detect bright points in the quiet-Sun region. The time sequence of these images is not evenly distributed across the observational period: a group of 2–6 images are taken with only $\sim$ 10-min cadence but adjacent groups are usually separated by a time gap of 2–4 hours, mostly due to satellite nights.

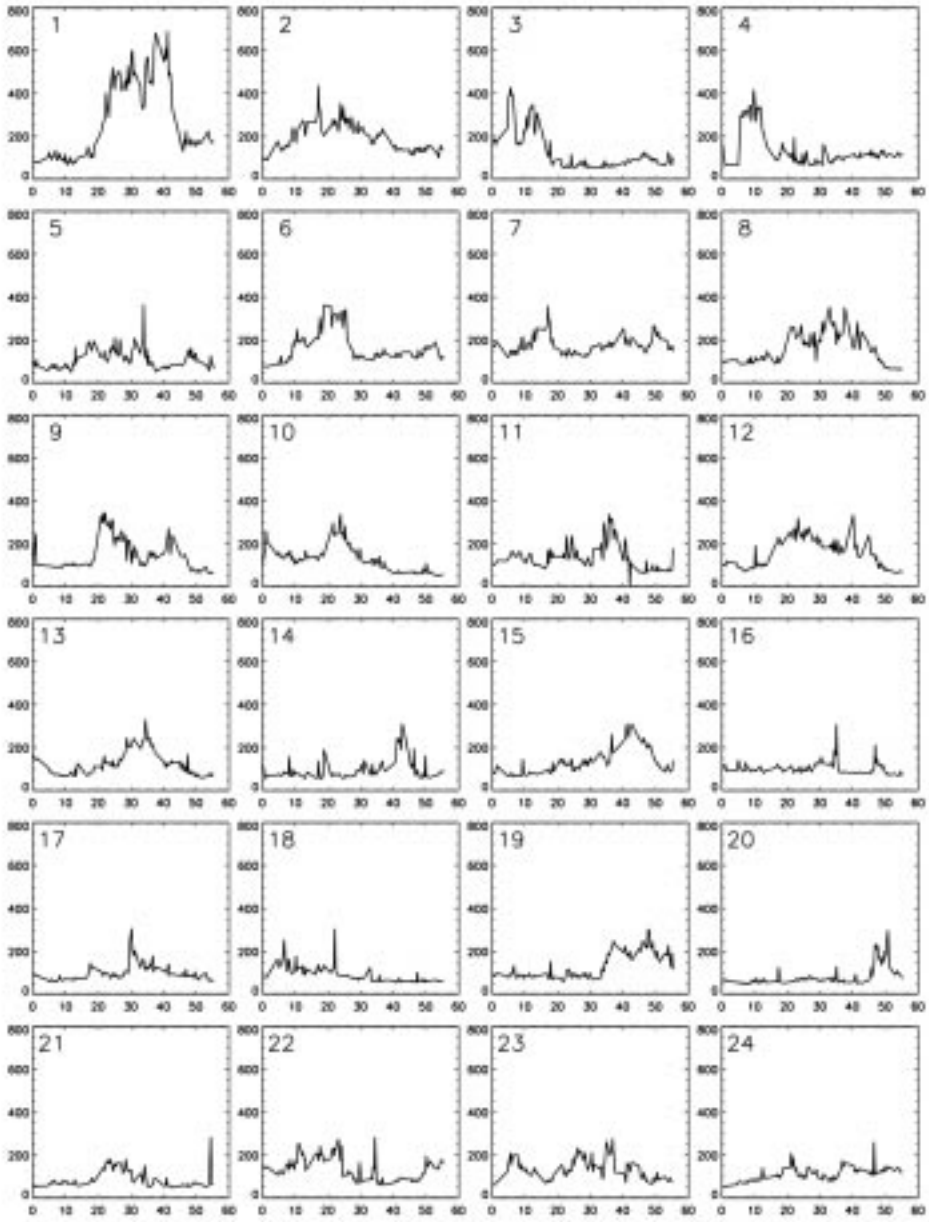

Figure 8. Time profiles of the flux of the peak pixel of 24 strong BPs identified with full life cycle tracks. The X-axis and Y-axis denote a time range of 60 hours, and a flux range of 800 DN s $^{-1}$ pixel^{-1} for all 24 events, respectively. The number in the top-right of each panel (numbered 1 to 24) indicates the numbering of BPs in Figure 5 which shows their location. Note that the numbering is in the order of descending strength of BPs at their peak.

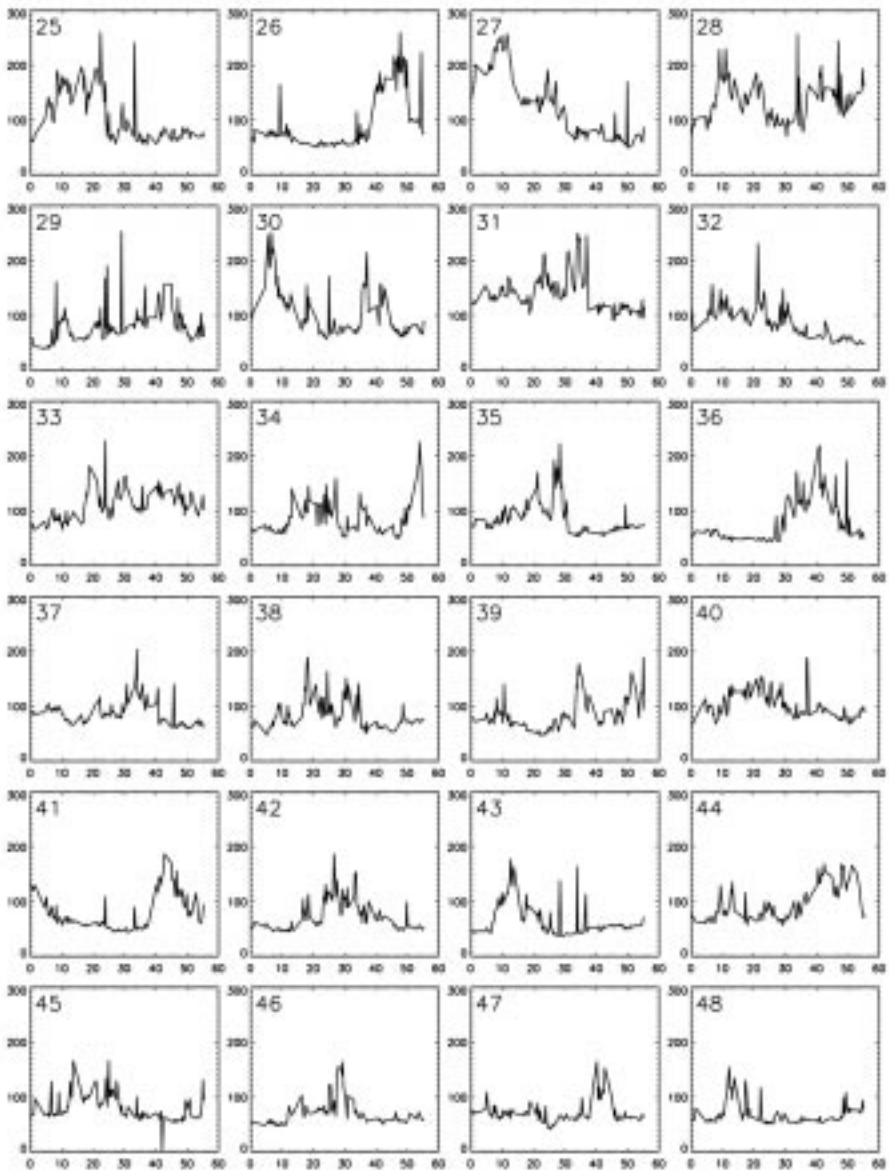

Figure 9. Time profiles of the flux of the peak pixel of 24 weak BPs identified with full life cycle tracks. The X-axis and Y-axis denote a time range of 60 hours, and a flux range of 300 DN s $^{-1}$ pixel^{-1} for all 24 events, respectively. The number in the top-right of each panel (numbered 25–48) indicates the numbering of BPs in Figure 5 which shows their location. Note that the numbering is in the order of descending strength of BPs at their peak.

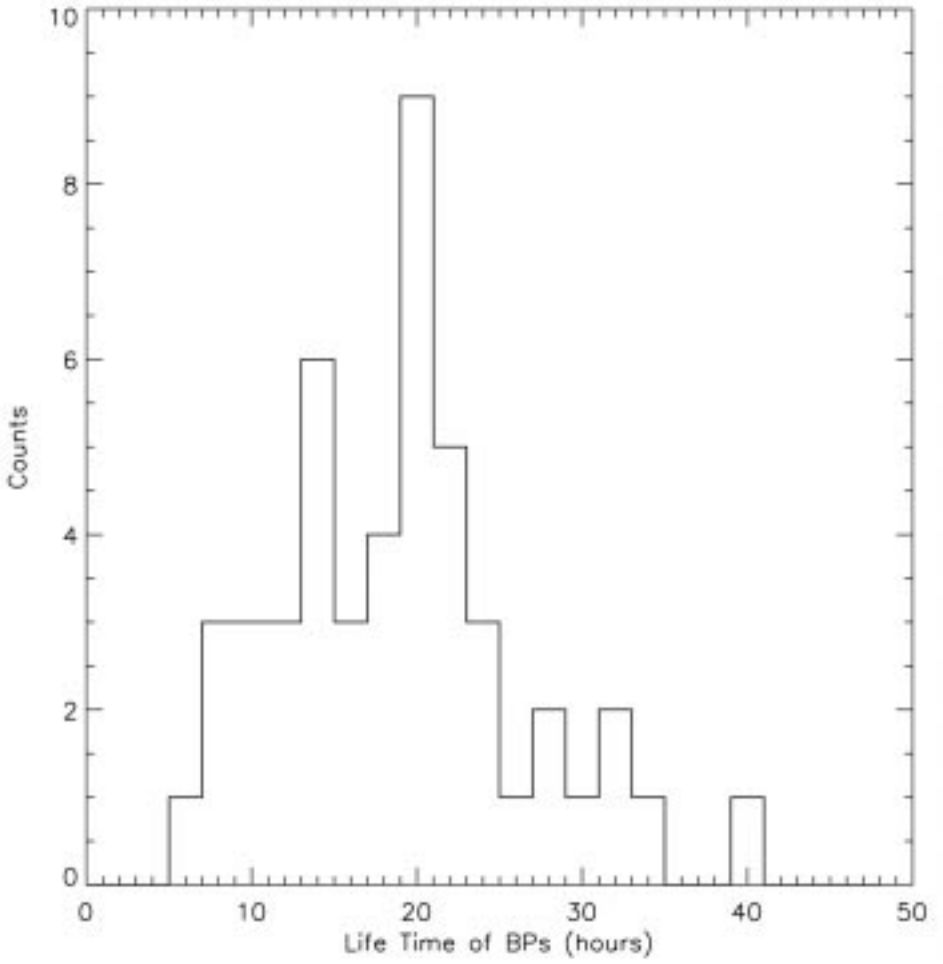

Figure 10. Histogram of the lifetime of 48 BPs with full life cycle track. The bin size is 2 hours.

The number of BPs seen in SXT soft X-ray images is much smaller than that seen in EIT 195 Å images. We identify only one BP in SXT for every three or four BPs seen in EIT using the same intensity threshold (3σ for both cases). For instance, there are 12 BPs in the SXT thin Al image taken at 20:56 UT, 11 November, and 12 BPs in the SXT AlMg image taken at 20:58 UT, 11 November, while in the same field of view there are 41 BPs in the EIT image taken at 20:57 UT, 11 November. Regarding the spatial coverage, in both thin Al and AlMg SXT images 0.8% of the quiet-Sun area is covered by BPs, while in an EIT 195 Å image 1.4% of the quiet-Sun area is covered by BPs.

We also compare the temporal evolution of BPs in SXT images with that in EIT 195 Å images. In Figure 11, the time profiles of the four strongest BPs, events

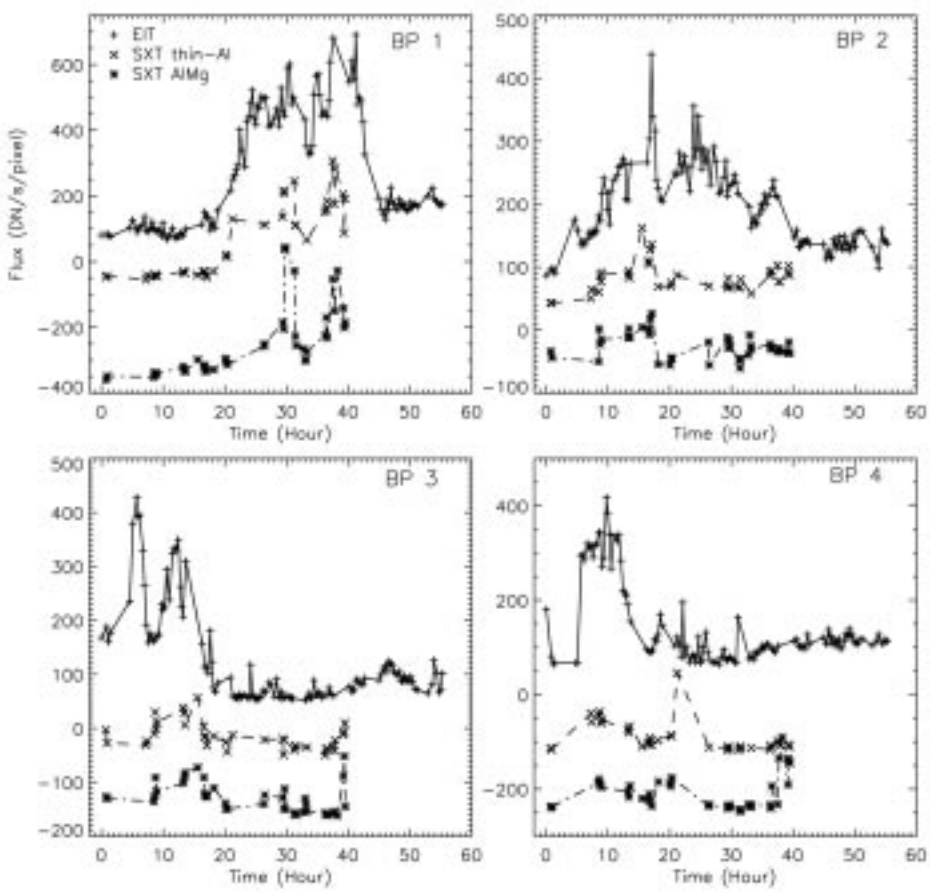

Figure 11. Time profiles of peak pixel flux of four strongest BPs (panels 1, 2, 3, and 4, respectively) in EIT (denoted by $+$), SXT thin Al (denoted by $\times$) and SXT AlMg (denoted by $*$). Note that the flux value on the Y-axis refers to EIT observations, while the SXT curves have been adjusted vertically in order to separate the curves: in this figure, we are only interested in the temporal variation at different wavelengths, not in absolute flux levels.

1, 2, 3, and 4 whose positions are indicated in Figure 5, are plotted in panels 1, 2, 3, and 4, respectively. In each panel, we display the time profile of peak pixel flux of the corresponding BP seen in EIT 195 Å, SXT thin Al and SXT AlMg, respectively. Note that the flux value on the Y-axis refers to the EIT observations; the SXT curves have been adjusted vertically in order to clearly display the curves. In general, the flux variation of SXT BPs follows their EIT counterparts, especially during the strong brightening phase. Each peak phase in a SXT profile almost always has a counterpart in the corresponding EIT profile. The unusual peak of SXT thin Al time profile of BP 4 (lower-right panel) may be due to instrumental contamination by a spurious spike. On the other hand, during the weak brightening

phase of a BP in EIT 195 Å, the BP may be barely visible as a BP in SXT. As a result, the lifetime of a BP appears to be shorter in SXT than that in EIT 195 Å. Note that we have not measured and given the exact value of the lifetime of BPs in SXT due to the large uncertainty in determining the starting and ending time of a BP in the irregular SXT sequence.

4. Discussion

The mean lifetime of 20 hours of BPs in EUV we determine is much longer than that of 8 hours determined by Golub *et al.* (1974) for BPs in X-ray. We believe that 20 hours is the realistic average lifetime of BPs. The shorter lifetime seen in X-rays is simple due to the fact that a BP has a low coronal temperature for most of its lifetime during which it does not give rise to enough X-ray emission to be detected. This explanation is supported by the results presented in the last section of this paper in that simultaneous observations show smaller numbers and shorter life times for BPs observed in soft X-rays by SXT than in EUV 195 Å by EIT. BPs may be mostly composed of plasma with temperature from 1 to 2 MK, which is more favorably observed in EUV than in soft X-rays. Only during some phases, e.g., flaring phases during which a significant amount of plasma is heated to above 2.5 MK, does a BP become visible in soft X-rays. The longer lifetime of BPs is more consistent with recent statistical results on quiet-Sun magnetic field evolution, which is found to be replenished by newly emerging flux in about 40 hours (Schrijver *et al.*, 1998). It is generally believed that coronal features, including BPs, are driven by the underlying magnetic field. Detailed studies of several individual BPs also reveal that the evolution of BPs from birth to decay is extremely well correlated with the rise and fall of photospheric magnetic field (Pres and Phillips, 1999).

Superposed on the long-term evolution of BPs, there are many spiky components which indicate the intermittent nature of BPs. Spiky components correspond to transient brightenings which have been reported in many earlier studies (Sheeley and Golub, 1979; Habbal and Withbroe, 1981; Habbal, Dowdy, and Withbroe, 1990; Strong *et al.*, 1992; Krucker *et al.*, 1997; Benz and Krucker, 1999; Shimojo and Shibata, 1999); those fast cadence observations reveal that transient brightenings usually have a lifetime of 5 to 20 min. Transient brightenings are suggested to originate from micro-flares, since their lifetime is consistent with the cooling time of impulsively heated coronal plasma. Fast cadence multiple wavelength observations of BPs, which cover the temperature range of the corona, transition region and chromosphere, are particularly useful in diagnosing the nature of transient brightenings (Habbal, Dowdy, and Withbroe, 1990; Benz and Krucker, 1999). Unfortunately, our data set, with a temporal resolution of 26 min (longer than the typical life-time of transient brightenings) does not allow us to study the transient brightenings in detail.

Regarding the relationship between transient brightenings or rapid fluctuations of BPs (5–20 min) and the long-term evolution of BPs ($\sim$ 20 hours), an important question is whether the long-term trend is an integrated effect of many individual but overlapping transient brightenings, or it is contributed by a fundamentally different heating source. We cannot answer this question with this data set. But we emphasize that there must be some mechanism that controls the long term evolution of BPs. This property of BPs would be a further constraint on theoretical models of BPs.

Our measurements of the spatial distribution of BPs indicate that BPs occupy a rather small part of the quiet-Sun region: only 1.4% of the area, using a 3σ threshold in EIT 195 Å images, and an even smaller area in SXT images. These numbers are consistent with the measurements by Falconer *et al.* (1998) who gave a spatial coverage of $\sim$ 2% for BPs in EIT 195 Å images. Early studies by Habbal and Grace (1991) using *Skylab* observations presented a coverage of 10% to 25% for various EUV lines; these relatively larger numbers may arise from the cooler EUV lines used and different intensity threshold adopted. Nevertheless, all the numbers agree that BPs occupy a small part of quiet-Sun region. As a result, the quiet-Sun regions are not energetically dominated by BPs. The BPs contribute only about 5% of the total emission from quiet-Sun regions in EIT 195 Å observations. This supports the suggestion that BPs alone may not provide sufficient energy to heat the quiet corona (Habbal and Grace, 1991).

5. Conclusion

By continuously tracking a quiet-Sun region of size $780'' \times 780''$ over a period of 55 hours using EIT observations of Fe XII 195 Å and soft X-ray observations from SXT, we have carried out statistical studies of the spatial distribution and temporal evolution of coronal bright points. The histogram of flux for all pixels in the EIT 195 Å images shows that the enhanced flux part which corresponds to BPs has a power-law distribution, while the lower flux part which corresponds to the dominant quiet-Sun region has a Gaussian-like distribution; The two parts are separated at a flux level of 3σ above the average quiet-Sun flux. Using this 3σ threshold, we find on average one BP every 90 Mm $\times$ 90 Mm area, or equivalently 800 BPs on the whole solar surface at any moment. The average size of a BP is 110 Mm^2. It turns out that only 1.4% of the quiet-Sun area is occupied by BPs. The flux from all BPs contributes only 5% of the total flux from the quiet Sun. This indicates that the quiet Sun is not heated by BPs.

In the 55-hour period of EIT observations, we identify 48 BPs whose full life cycle can be tracked from their initial appearance to final disappearance. Thirty-six out of the 48 BPs have a lifetime lying between 10 and 30 hours. The average lifetime of the BPs is 20 hours, which is much longer than the previously reported 8 hours based on *Skylab* X-ray observations (Golub *et al.*, 1974). The lifetime of

these BPs derived from simultaneous SXT soft X-ray observations also appears shorter than that in EIT 195 Å observations. The number of BPs found in SXT images is also smaller than that in EIT images. The differences can be attributed to the typical coronal temperature of BPs (< 2 MK) which allow them more favorably to be observed at EUV than at soft X-ray wavelengths.

Acknowledgements

This research was supported by NASA grants NAG-5-8192, NAG-5-7901, NAG-5-7370, and NSF grants ATM 96-12738 and ATM 99-09809. We thank Alexander Nindos for valuable discussions. We also thank the referee for valuable comments.

References

Benz, A. O. and Krucker, S.: 1999, *Astron. Astrophys.* **341**, 286.
Delaboudinière, J.-P. *et al.*: 1995, *Solar Phys.* **162**, 291.
Falconer, D. A., Moore, R. L., Porter, J. G., and Hathaway, D. H.: 1998, *Astrophys. J.* **501**, 386.
Golub, L., Krieger, A. S., Silk, J. K., Timothy, A. F., and Vaiana, G. S.: 1974, *Astrophys. J.* **189**, L93.
Habbal, S. R.: 1992, *Ann. Geophys.* **10**, 34.
Habbal, S. R. and Grace, E.: 1991, *Astrophys. J.* **382**, 667.
Habbal, S. R. and Withbroe, G. L.: 1981, *Solar Phys.* **69**, 77.
Habbal, S. R., Dowdy, J. F., Jr., and Withbroe, G. L.: 1990, *Astrophys. J.* **352**, 333.
Harvey, K. L.: 1996, in R. D. Bentley and J. T. Mariska (eds.), *Magnetic Reconnection in the Solar Atmosphere, ASP Conference Series*, Vol. 111, 9.
Harvey, K. L., Harvey, J. W., and Martin, S.F.: 1975, *Solar Phys.* **40**, 87.
Kankelborg, C. C., Walker, A. B. C., Jr., Hoover, R. B., and Barbee, T. W., Jr.: 1996, *Astrophys. J.* **466**, 529.
Krucker, S., Benz, A. O., Bastian, T. S., and Acton, L. W.: 1997, *Astrophys. J.* **488**, 499.
Kundu, M. R., Raulin, J. P., Pick, M., and Strong, K. T.: 1995, *Astrophys. J.* **444**, 922.
Longcope, D. W.: 1998, *Astrophys. J.* **507**, 433.
Pres Pawel and Phillips, K. J. H.: 1999, *Astrophys. J.* **510**, L73.
Priest, E. R., Parnell, C. E., and Martin, S. F.: 1994, *Astrophys. J.* **427**, 459.
Sheeley, N. R., Jr. and Golub, L.: 1979, *Solar Phys.* **63**, 119.
Shimizu, T.: 1995, *Publ. Astron. Soc. Japan* **47**, 251.
Shimojo, M. and Shibata, K.: 1999, *Astrophys. J.* **516**, 934.
Schrijver, C. J. *et al.*: 1998, *Nature* **394**, L152.
Strong, K. T., Harvey, K. L., Hirayama, T., Nitta, N., Shimizu, T., and Tsuneta, S.: 1992, *Publ. Astron. Soc. Japan* **44**, L161.
Tsuneta, S., Acton, L., Bruner, M., Lemen, J., Brown, W., Caravalho, R., Catura, R., Freeland, S. *et al.*: 1991, *Solar Phys.* **136**, 37.
Vaiana, G. S. *et al.*: 1973, *Astrophys. J.* **185**, L47.
Webb, D. F., Martin, S. F., Moses, D., and Harvey, J. W.: 1993, *Solar Phys.* **144**, 15.